

Construction and Simulation of a Planar Transformer Prototype

Sebastián Guarín; Sergio Velarde; Edwin Castaño; and Alexander Molina-Cabrera 

DOI: <https://doi.org/10.32397/tesea.vol2.n2.1>

Research paper

Received: 15 April 2021; Accepted: 22 October 2021; Published: 15 December 2021

Abstract—This paper illustrates the design and building of a planar transformer prototype with a 1:1 transformation ratio for high-frequency applications in power electronics. By using reference literature and considering the ferrite core dimensions, the windings were conceived and exported to Gerber format using PCB design software. The transformer prototype was then assembled and tested under laboratory conditions for frequencies from 800 Hz to 5 MHz, which showed a sinusoidal wave at the transformer output from 1.3 kHz onwards and a better performance starting at 10 kHz, where the losses were significantly reduced and the transformation ratio was closer to the originally designed. As a final step, a finite element method (FEM) analysis was carried out to understand the electromagnetic flux behavior using a 3D Multiphysics simulation software. The 3d building process and details are explained step by step and the resulting magnetic flux density is graphically shown for the core and the windings.

Index Terms—Planar transformer; experimental validation, High-frequency applications; 3D simulation.

I. INTRODUCTION

CLIMATE change has motivated the rise of new ways to generate energy such as solar panels and wind power. Renewable energy operation is tightly linked with the weather; thus, it needs more robust systems that will not necessarily be in the classic generation – transmission – distribution schema. Smart Grids and distributed generation make part of these relatively new ways of producing energy that, as much as the conventional generation methods, require power conversion systems [1], [2]. In the traditional way, conventional transformers handle the conversion process. Conversely, Smart Grids require power converters, which typically work at high frequencies and include devices known as planar transformers (PT) [3].

Planar transformers are widely used in fields such as the aeronautics and spatial industries with applications in electrical mobility, medicine, defense and embedded systems, etc. Its compact shape and high-density properties represent fundamental characteristics for its use within electronic circuits and, more particularly, for high frequency power converters. Additionally, PTs present unique advantages such as low profile, outstanding thermal behavior, modularity, and simple

manufacturing that result attractive for the aforementioned fields [1], [4], [5].

There are two fundamental characteristics that mark the difference between the Planar and classic transformer: The geometry of the core and the structure of the windings [6]. The planar transformer core is typically made of soft Ferrite, due to its high magnetic permeability, low electrical conductivity, and comparatively low losses at high frequencies. In the other hand, its windings are commonly made with PCBs. This allows the designer to have more flexibility and precision on the final design with the required specifications, according to [7]. The main reasons that motivated the development of the planar transformer relied on the need to miniaturize power-handling components such as the transformer itself [8], [9], mostly for high frequency and high-power density usage. This reduction in size and format, would simplify a low-profile assembly, making it adaptable to a low-cost mass production, contrary to the conventional transformer [10].

One of the first existing planar device records dates from 1967, a transmission-line transformer was designed with an etched geometry to improve thermal behavior and bandwidth ratio. In 1986, A. Estrov in [11] patented a “Switching electrical power supply utilizing miniature inductors integrally in a PC”. This development greatly simplified the study of planar devices. Articles [7], [8] have been increasingly written on different aspects of the planar transformer. In 1988 a study was conducted on magnetic and insulating thin films fabricated on substrates using thin film deposition techniques. Later, the authors of [12] in 2004 the integration with resonant circuits was developed, Linkage Flux Path (LFP) and known core shapes are studied in new core shapes and winding structures. In 2010, authors of [13] an optimal design study was proposed with an improved interleaving structure that minimizes AC resistance, leakage inductance and stray capacitance. And more recently, references [14], [15] in 2014, has studied the trade-off between power losses and frequency at high levels, results are compared using the Dowell method. On the other hand, in [16], a PT with a novel topology (Meander-type) is designed, fabricated and later improved on [17]. Finally, in 2018, another topology is proposed on [18] in form of a Multilayer Planar Pot-Core Transformer with high efficiency.

Although there exist a broad range of specific studies with specific applications, to our knowledge, there is not an approach of the basic construction parameters of a simple planar transformer that analyses it from an educational per-

S. Guarín, S. Valverde, and E. Castaño are with Master Program in Electrical Engineering, Universidad Tecnológica de Pereira, Pereira 660003, Colombia; (email: {sebas1302.galeanoe}@utp.edu.co)

A. Molina-Cabrera is with Facultad de Ingeniería, Universidad Tecnológica de Pereira, Pereira 660003, Colombia.; (email: almo@utp.edu.co)

spective. Therefore, in this paper, a low-cost planar transformer prototype was conceived with a 1:1 transformation ratio (3 winding turns on each side) and the usage of accessible components to simplify its construction and show the basic characteristics of its behavior through a laboratory test and a simulation. Every step is shown and explained so as to encourage students from engineering and other related fields to better understand this device by a practical manipulation and hands-on experimentation. This paper is organized as follows: succeeding the Introduction, Section II explains the construction of the prototype divided on Core, Windings and Assembly, Section III focuses on the experimental results, Section IV provides the tridimensional simulation and shows its results. Finally, Section V exposes the conclusions.

II. CONSTRUCTION OF THE PROTOTYPE

The construction of the transformer comprises 3 main steps: the core, the windings, and their assembly. Figure 1 depicts a flow diagram that contains an overview of the construction and testing of the device, in which those 3 steps are in yellow, blue, and red, respectively.

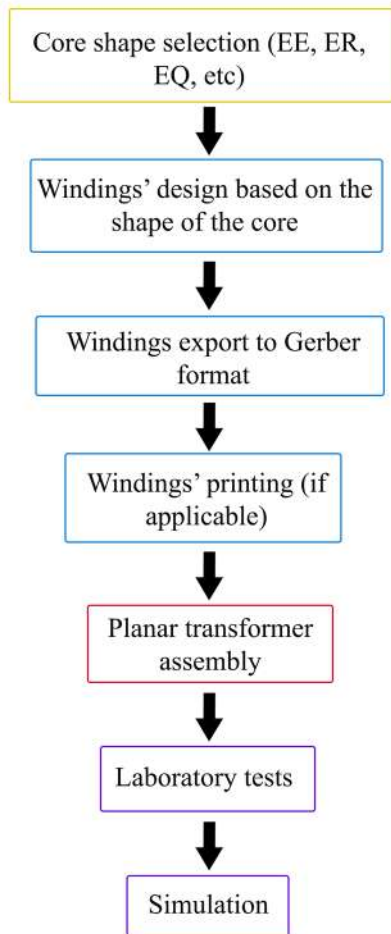


Fig. 1. Construction and testing flowchart.

A. Core

The Ferrite core has different shapes depending on the final application, it is often chosen based on the desired magnetizing inductance and active power through its area product. Although in nowadays industry the core can be completely personalized, there are 4 shapes that are often available in the market (see Figure 2): EE, ER, EQ and PQ [7], [19], [20].

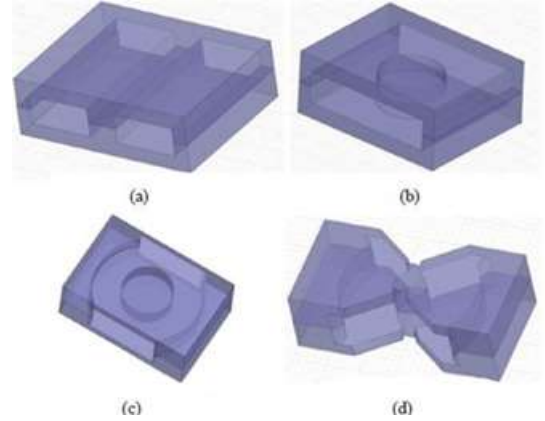


Fig. 2. Type of cores: (a) EE, (b) ER, (c) EQ and (d) PQ core shapes [19].

A ferrite EQ core was used for the construction of the prototype, with the dimensions shown in Figure 3.

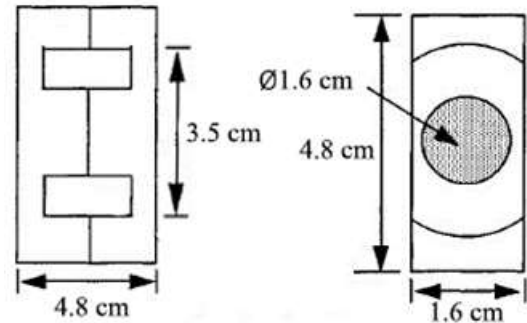


Fig. 3. Type of cores: (a) EE, (b) ER, (c) EQ and (d) PQ core shapes [19].

The cost of one core unit, on the local market, was of \$0.5 approx. This core shape was chosen due to its round center post, which allows a more efficient use of copper in the windings and board space, and in consequence reduced copper losses [7]. The power losses on the core can be neglected, due to the high resistivity of the ferrite [21]. On the other hand, the hysteresis losses are defined as a non-linear function of the frequency and the maximum magnetic flux, as follows:

$$P_{hys} = K_c (DB)^m f_s^n, \quad (1)$$

where P_{hys} is the hysteresis losses per unit volume, DB is the magnetic flux density swing, f_s is the switching frequency, m corresponds to a construction constant in the range of 2 to 3, n is a construction constant in the range of 1 to 2, and K_c represents the core loss constant.

B. Windings

Planar windings have important advantages over the conventional wiring, they are less bulky and easier to manufacture, and thus, easier to integrate and embed to the final application [15]. There are several types of planar windings, among them:

- Lead Frame: Particularly useful for low voltage – high current applications, due to its width. They typically have only one turn, which fits the core [6].
- PCB: Printed Circuit Board, the most common planar winding type. Useful for high voltage – low current applications. It can be found in a single layer or can be designed as multi layers [6], [7].
- Meander Type: The windings are engraved into the ferrite core to reduce overall transformer thickness [17].

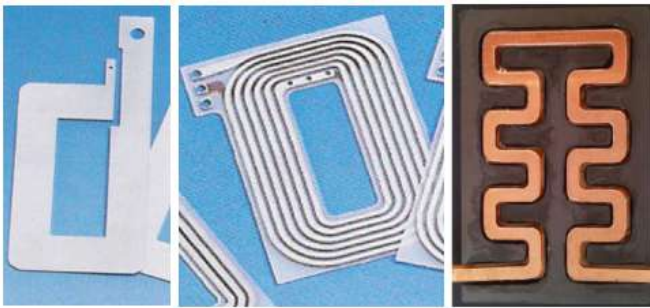


Fig. 4. Examples of Leadframe (left), PCB (center) and Meander type (right) [6], [17].

Just as for the core, the final application is the determining factor when choosing a winding configuration. For the present study, and due to its relatively easy design and implementation, the PCB type was chosen. As a first design step, the space between the center column and the outer ones was calculated to decide how many turns the transformer would have. For this purpose, both the diameters of the inner and outer circle were calculated, the difference was 1 cm. On the Planar Transformer Handbook, one of the proposed transformers has 2.54mm of trace width, and a winding resistance of 0.057Ω , a similar width was selected based on their proposal: 2.2mm for it to have enough space for three turns on each board [7]. The windings were drawn on Adobe Illustrator as shown in Figure 5.

The external holes on the corners (H1) allow to hold the structure with M6x50mm screws. The blue holes on the trace ends (H2) are used for the internal connections between the windings, they were designed with a 2mm diameter for it to fit up to 13-gauge copper wire. These holes have copper around them for the welding to be simpler. The 4 blue holes on the board (H2), with the same characteristics, serve as the transformer input and output, and along with the black hole next to the trace (H3), they also make the internal connection easier as explained on Fig. 8. Once the Illustrator vector was finished, it was exported to the PCB design Software Fritzing on five layers that the program requires to identify the PCB structure:

- Copper Top
- Copper Bottom

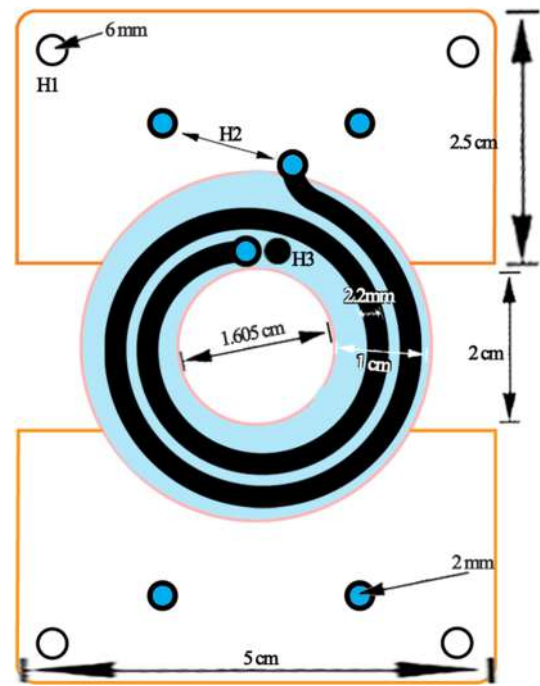


Fig. 5. Winding design.

- Silkscreen Top
- Silkscreen Bottom
- PCB Base

This software was selected because of its intuitive interface, free license, capability to import vector files (.svg) and certainly, to export as Gerber format (.gbr), which contains the necessary information for PCB printing. The designer can use it for implementing his/her own design strategy. We used the services of JLCPCB, in China, for printing the windings. This company requires the files in Gerber format, which is another important reason to have chosen Fritzing.

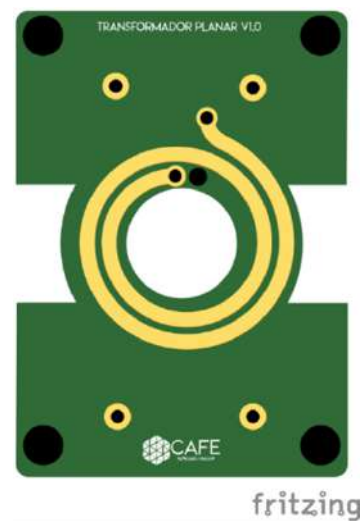


Fig. 6. Final PCB design.

The file was then uploaded to the JLCPCB platform, and the order was placed: Five panels of 152mm*150mm containing

6 windings boards each, as shown in Fig. 7. The total cost of the order, including shipping to Colombia, was of \$18.2. As only six were used to assemble the final structure, the cost for this application was \$3.64.



Fig. 7. Panel of 6 winding boards.

C. Assembly

Figure 8 explains the connection of the windings, in which spot welding was used on the copper wire with tin. The current follows the path from the “Primary winding input” towards the “primary winding output”, likewise for the secondary winding. As depicted, the current on the primary winding has the opposite direction in relation to that of the secondary winding.

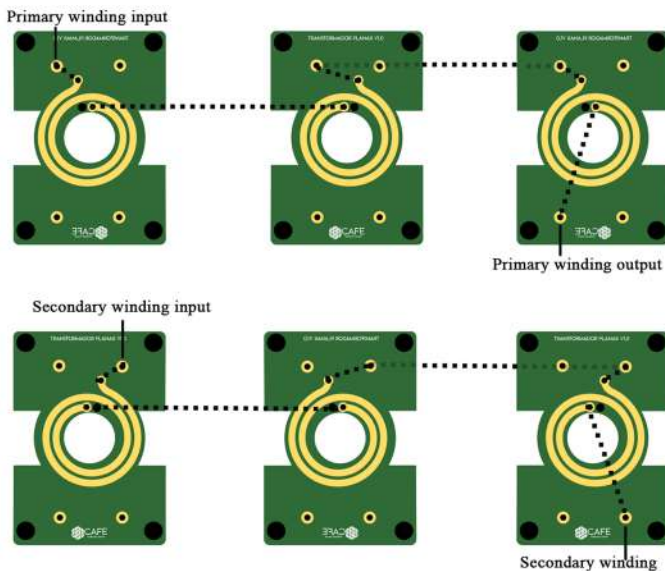


Fig. 8. Winding connection.

The winding boards can be interleaved or non-interleaved. The first means the primary and the secondary boards can be

stacked one directly after the other, this is usually written as PS-PS-PS (for 6 winding boards) where P stands for Primary and S stands for Secondary. This is however not the only type of interleaving, as an example, for an 8 winding boards stacking, an interleaving of PP-SS-PP-SS can be performed. Non-interleaved configuration for an 8 boards stacking is PPPP – SSSS. Nonetheless, the latter arrangement presents more losses due to the skin and proximity effects that cause the current density to be non-uniform at high frequencies [19]. In [15] an interleaved arrangement of 8 boards is presented, it is shown that AC resistance decreases as the frequency increases.

For this study, an assembly of 6 boards was selected due to the available space within the core, considering the dimensions of the M6 screw nuts which were used not only to adjoin steadiness to the structure but also to create a bigger gap between the windings and thus, reduce the proximity effect. A PPP-SSS arrangement was chosen for it simplifies the manual inner connection. The hole on H3, was nonetheless designed to create in a simpler way an interleaved manual connection for future developments.

As stated in the beginning of this section, the interconnections were made with 14-gauge copper wire, using spot welding with tin. The structure was held with M6 screws used on the border holes (H1) and M6 screw nuts were used to guarantee structural stability. With the winding board connections done, the core was inserted and secured with plastic moorings. Outer copper wire was intentionally left to connect the primary and secondary inputs and outputs to the laboratory devices.



Fig. 9. Transformer assembly completed.

III. EXPERIMENTAL RESULTS

So as to evaluate the power transfer of the transformer, a signal generator, an oscilloscope and a multimeter were used. It is important to mention that before the behavior evaluation, a conductivity test was executed using the multimeter to make sure there were no contact points that might cause the output signal to be the same as the input signal, or worse, that could provoke a short-circuit. Figure 10 depicts the connection of the transformer to measuring instruments.

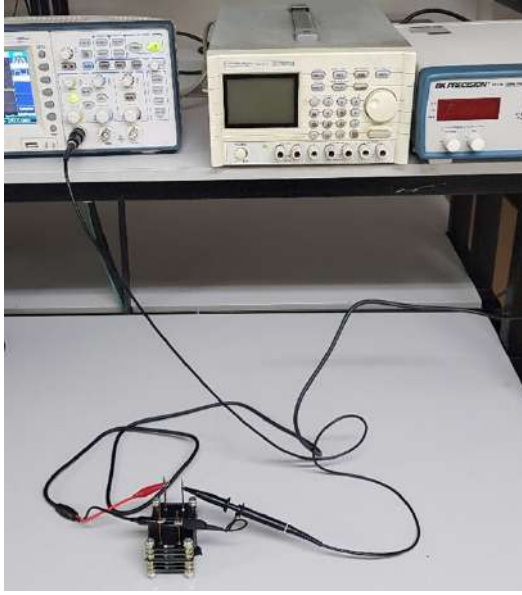


Fig. 10. Experimental evaluation: connection of the transformer to the oscilloscope (left) and to the signal generator (right).

The primary is then excited with a low frequency sinusoidal signal that is gradually increased until the oscilloscope's screen starts showing another sinus-like signal, which happens around 1.3 kHz. From this point on, screenshots are progressively taken with the aim of displaying the device behavior (see Figure 11).

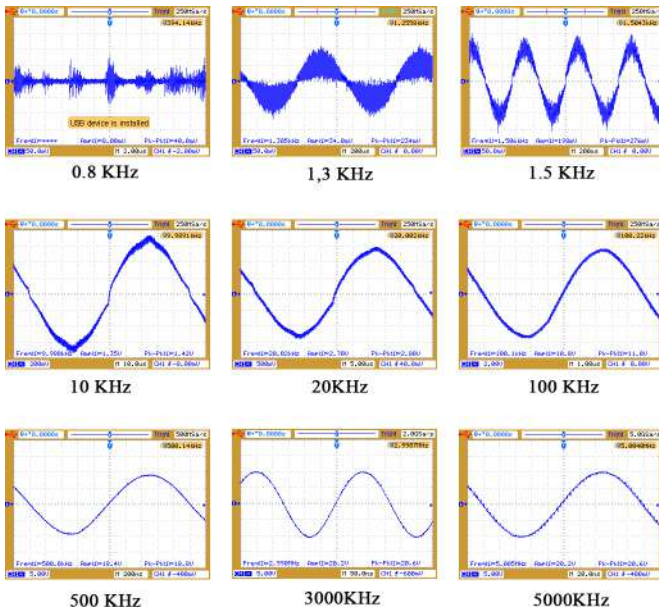


Fig. 11. Experimental results: Signal on the transformer output at increasing frequencies.

The signal generator output was configured to provide the maximum value of voltage: 5V. As for the frequency, measurements were made from 800 Hz up to the device's limit: 5 MHz. During the test, voltages at the primary (V_p) and secondary (V_s) of the transformer were measured using the oscilloscope and tabulated as shown in Table I.

TABLE I
VP AND VS FOR DIFFERENT FREQUENCIES.

Frequency	VP (V)	Vs (V)	Transformation Ratio
0.8	0.072	0.200	2.78
1.3	0.068	0.064	0.94
1.5	0.076	0.068	0.89
10	3.440	4.080	1.19
20	2.400	3.440	1.43
50	2.480	2.320	0.94
100	2.500	2.360	0.94
200	2.080	2.000	0.96
500	2.650	2.400	0.91
1000	3.200	3.120	0.98
3000	2.960	3.200	1.08
5000	2.320	3.360	1.45

Figure 11 illustrates the power transfer results on the designed planar transformer. For frequencies from 10kHz onwards, the oscilloscope was configured with the single-period mode, to have a clearer depiction of the sinus wave. Starting at 1.3 kHz, a sinusoidal wave appears, and the transformation ratio is close to 1. Nevertheless, these low frequencies present higher losses. As Table I suggests, the transformer does not keep the designed transformation ratio under 10 kHz. The voltages on both primary and secondary of the transformer are greatly different from the one given by the source, is due to the flux leakage presented on the core for low frequencies. Above 10 kHz, the magnetic flux finds a lower reluctance path through the ferrite core than through the air, which results in less current consumption, a better flux linkage, and therefore, less losses. For these frequency values, the transformation ratio is almost 1:1, notably from 1000kHz to 3000 kHz range. The erratic behavior of the voltage at increasing frequencies is affected by the ferrite physical properties, the quality of the elements and the measuring process.

IV. TRIDIMENSIONAL SIMULATION

The main objective of this step is to observe the magnetic field behavior on the device. The simulation was conducted on COMSOL Multiphysics software and took about 13 hours on a computer with the following characteristics: 3.6 GHz Intel Core I7 processor, 8GB RAM and 64 bits Windows 10 OS. The 3D model was built with the real-life prototype dimensions, although in a simplified manner. This was necessary to reduce the structure complexity and focus the simulation on the magnetic behavior of the materials. The simplification was mainly performed in the windings, whose turns were represented as rings with the same width (2.2mm), as illustrated on Figure 12.

Three materials (taken from the COMSOL library) were used on the 3d geometry: Alloy Powder Core Ferrite for the core, Copper for the windings and Air for the surrounding environment. In a similar manner, three free tetrahedral meshes were generated for each component group, for the Air and for the core a "General physics" mesh was used, while for the windings a "Semiconductor" type was selected.

An electrical circuit was also adjoined to the simulation, so it could reproduce the voltage source and the losses on the windings. The first was selected with a 1 V amplitude at

60 Hz, while the resistances for the second had 0.01Ω for both the primary and secondary windings, this value was measured from the windings in the physical prototype.

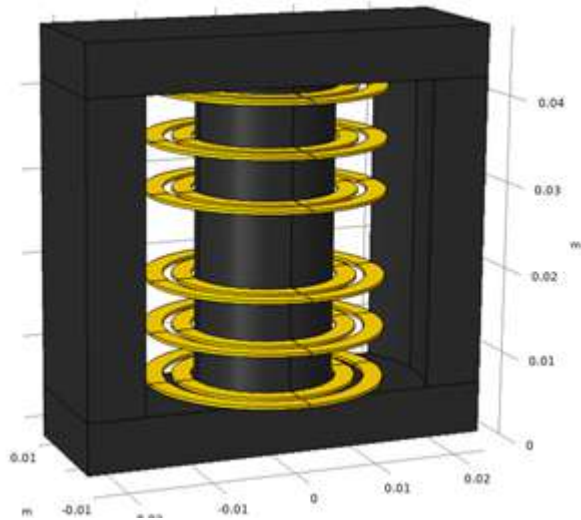


Fig. 12. Finished 3D PT Model

A. Simulation results

The fundamental study that was conducted is “Magnetic Fields” on the software interface. This study shows as result the magnetic field density on the geometry where it is performed and takes into consideration the materials, the selected electrical circuit (used to simulate the voltage source and the assigned losses on the windings), and the own magnetic restrictions of the device.

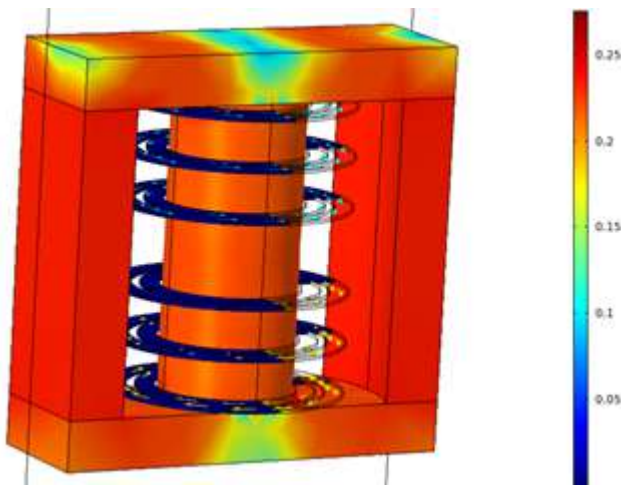


Fig. 13. This picture shows the magnetic flux density of the planar transformer on $t=0.05$ s, at 1 kHz and with 1 V input. As it can be seen, the core has a strong magnetic flux linkage in almost its whole surface, getting close to 0.25 T on the flashpoints. The arrows on the windings indicate the direction of the current.

V. CONCLUSIONES

A planar transformer prototype was built with a 1:1 transformation ratio, with 6 PCBs for the primary and secondary

windings, two turns each. The obtention, building, wiring, and design processes were explained for the core, windings, and connection elements. The finished prototype was then tested under laboratory conditions, where the power transfer was verified: under 10 kHz there were significant losses, while above that value the power transfer from primary to secondary presented a better behavior, notably at the range of frequencies from 1000 kHz to 3000 kHz, where the transformation ratio approached closely to the designed of 1:1.

The COMSOL Multiphysics software was used to perform the simulation considering the actual prototype size and the materials each component was made of, in order to observe the magnetic behavior of the transformer (especially the core), working at 1 kHz frequency with a 1V amplitude excitation. The resulting magnetic densities of the field had up to 0.25 T on the flashpoints.

This initial approach on this device mainly focused on its construction, design, and base characteristics. As future work, the prototype that was built is to be improved to reach the 1:1 transformation ratio. Studies can be conducted with different loads, at higher frequencies, on the power density, and the curves that characterize it. Other prototypes can be built changing parameters as the number of PCB windings, the distance between them, the number of their turns, the transformation ratio, and different interleaving configurations. As for the simulation, it is important to improve the geometry by a more realistic approach that allows to analyze the voltages, currents, and power both at the input and output of the device, and furthermore, the behavior under different loads.

REFERENCES

- [1] Z. Ouyang, O. C. Thomsen, and M. A. E. Andersen, “Optimal Design and Tradeoff Analysis of Planar Transformer in High-Power DC–DC Converters,” *IEEE Transactions on Industrial Electronics*, vol. 59, pp. 2800–2810, jul 2012.
- [2] F. M. Serra and C. H. D. Angelo, “Control of a battery charger for electric vehicles with unity power factor,” *Transactions on Energy Systems and Engineering Applications*, vol. 2, pp. 32–44, jul 2021.
- [3] S. Dhivya and R. Arul, “Demand Side Management Studies on Distributed Energy Resources: A Survey,” *Transactions on Energy Systems and Engineering Applications*, vol. 2, pp. 17–31, July 2021.
- [4] W. Chen, Y. Yan, Y. Hu, and Q. Lu, “Model and design of PCB parallel winding for planar transformer,” *IEEE Transactions on Magnetics*, vol. 39, pp. 3202–3204, sep 2003.
- [5] C. Quinn, K. Rinne, T. O'Donnell, M. Duffy, and C. Mathuna, “A review of planar magnetic techniques and technologies,” in *APEC 2001. Sixteenth Annual IEEE Applied Power Electronics Conference and Exposition (Cat. No.01CH37181)*, IEEE, 2001.
- [6] S. Ben-Yaakov, “The benefits of planar magnetics in of power conversion planar magnetics (pm) : The technology that meets the challenges of hf switch and resonant mode power conversion,” 2006.
- [7] C. W. T. McLyman, *Chapter 20: Planar Transformers in Transformer and Inductor Design Handbook*. CRC Press, dec 2017.
- [8] E. Rodriguez and A. Estrov, “Switching electrical power supply utilizing miniature inductors integrally in a pcb,” Nov. 1984.
- [9] E. de Jong, E. de Jong, B. Ferreira, and P. Bauer, “Toward the Next Level of PCB Usage in Power Electronic Converters,” *IEEE Transactions on Power Electronics*, vol. 23, pp. 3151–3163, nov 2008.
- [10] A. Estrov, “Low-profile planar transformer for use in off-line switching power supplies,” Apr. 1991.
- [11] R. Drapeau, “A wide bandwidth, high-ratio, planar transmission-line transformer for use at cryogenic temperatures,” *IEEE Transactions on Magnetics*, vol. 3, pp. 64–71, mar 1967.

- [12] O. Oshiro, H. Tsujimoto, and K. Shirae, "Structures and Characteristics of Planar Transformers," *IEEE Translation Journal on Magnetics in Japan*, vol. 3, pp. 543–544, jul 1988.
- [13] J. Biela and J. Kolar, "Electromagnetic integration of high power resonant circuits comprising high leakage inductance transformers," in *2004 IEEE 35th Annual Power Electronics Specialists Conference (IEEE Cat. No.04CH37551)*, IEEE, 2004.
- [14] T. A. Pereira, F. Hoffmann, P. K. Prasobhu, M. Liserre, V. Golev, J. Schnack, and U. Schumann, "Optimal Design of Planar Transformer for GaN based Phase-Shifted Full Bridge Converter," in *2020 IEEE Applied Power Electronics Conference and Exposition (APEC)*, IEEE, mar 2020.
- [15] A. Ammouri, H. Belloumi, T. B. Salah, and F. Kourda, "High-frequency investigation of planar transformers," in *2014 International Conference on Electrical Sciences and Technologies in Maghreb (CISTEM)*, IEEE, nov 2014.
- [16] S. Djuric, G. Stojanovic, M. Damjanovic, M. Radovanovic, and E. Laboure, "Design, Modeling, and Analysis of a Compact Planar Transformer," *IEEE Transactions on Magnetics*, vol. 48, pp. 4135–4138, nov 2012.
- [17] S. M. Djuric and G. M. Stojanovic, "A Compact Planar Transformer With an Improved Winding Configuration," *IEEE Transactions on Magnetics*, vol. 50, pp. 1–4, nov 2014.
- [18] F. Alam, Z. Ullah, A. Majid, J. Saleem, and A. Haider, "Design of high frequency (MHz) planar pot-core transformer," in *2018 1st International Conference on Power, Energy and Smart Grid (ICPESG)*, IEEE, apr 2018.
- [19] J. S. N. T. Magambo, R. Bakri, X. Margueron, P. L. Moigne, A. Mahe, S. Guguen, and T. Bensalah, "Planar Magnetic Components in More Electric Aircraft: Review of Technology and Key Parameters for DC–DC Power Electronic Converter," *IEEE Transactions on Transportation Electrification*, vol. 3, pp. 831–842, dec 2017.
- [20] Y.-H. Shin, Y.-S. Oh, K.-S. Ahn, and C.-S. Kim, "Adapter design using planar transformer for aircraft," in *INTELEC 2009 - 31st International Telecommunications Energy Conference*, IEEE, oct 2009.
- [21] C. L. Ebert, W. P. Carpes, and J. C. S. Fagundes, "Determination of magnetic losses in planar magnetic elements," in *2008 18th International Conference on Electrical Machines*, IEEE, sep 2008.



©2021 by the authors. Licensee TESEA, Cartagena, Colombia. This article is an open access article distributed under the terms and conditions of the Creative Commons Attribution (CC BY) license (<http://creativecommons.org/licenses/by/4.0/>)